



out external interference and the  $C/N_0$  taking into account the interfering system.

Following the ITU Recommendation M.1831, the signal-to-noise degradation experienced by a user in the presence of another interfering system is expressed as follows,

$$\Delta_{dB} = \left( \frac{C}{N_0 + P_0} \right)_{dBHz} - \left( \frac{C}{N_0 + P_0 + I_0} \right)_{dBHz} = \left( \frac{N_0 + P_0 + I_0}{N_0 + P_0} \right)_{dB} = \left( 1 + \frac{I_0}{N_0 + P_0} \right)_{dB}$$

where  $N_0$  is the thermal noise floor,  $P_0$  is intra-system interference, and  $I_0$  is the external interference. The external interference level is calculated as

$$I_0 [dBW/Hz] = G_{agg} [dB] + P_{max} [dBW] + SSC [dB / Hz] + L_x [dB]$$

$G_{agg}$  is the aggregate gain taking into account the interference introduced by all the satellites of one system in view.  $P_{max}$  is the maximum user received power, and  $SSC$  is the *spectral separation coefficient* between the interfering and the desired signals.  $L_x$  refers to any processing loss that might appear within the receiver.

The  $SSC$  is widely accepted by the GNSS community as an effective parameter used to characterize mutual interference, since it gives a measure of how the spectral shape of the interfering signal affects the performance of the receiver. The  $SSC$  definition is derived from the expression for the signal-to-noise-and-interference ratio (SNIR), which, for coherent early-late processing, is given as

$$SNIR = \frac{2TC_s \left[ \int_{-\beta_r/2}^{\beta_r/2} G_s(f) df \right]^2}{\int_{-\beta_r/2}^{\beta_r/2} G_w(f) G_s(f) df}$$

where  $T$  is the correlator period,  $C_s$  is the carrier power,  $\beta_r$  is the receiver front-end bandwidth,  $G_s(f)$  is the desired signal's power spectral density normalized to unit power over infinite bandwidth.  $G_w(f)$  is the power spectral density of the interference which can be decomposed into the sum of white noise and nonwhite interference, so that the previous expression becomes

$$SNIR = \frac{2TC_s \left[ \int_{-\beta_r/2}^{\beta_r/2} G_s(f) df \right]^2}{N_0 \int_{-\beta_r/2}^{\beta_r/2} G_s(f) df + C_i \int_{-\beta_r/2}^{\beta_r/2} G_i(f) G_s(f) df} \quad (1)$$

The effect of interference on the SNIR is given by the second term of the divisor, where the  $SSC$  is represented as

$$SSC = \int_{-\beta_r/2}^{\beta_r/2} G_i(f) G_s(f) df.$$

The  $SSC$  is also described in ITU-R M.1831, which considers the compatibility amongst various GNSS systems. For the

specific case of Galileo's potential interference with Globalstar, we assumed the following for the  $SSC$  calculation:

- The  $G_i(f)$  and  $G_s(f)$  of either the Galileo or Globalstar spectrum correspond to the theoretical spectra, truncated and normalized over a 16.5 megahertz bandwidth with respect to the interfering normalized over the infinite bandwidth of the victim  $G_s(f)$ . (See ITU-R M.1831.)
- Receiver bandwidth interference equal to one Globalstar FDMA channel width of 1.23 megahertz, for the worst case corresponding to the Globalstar channel closest to the main lobe of the Galileo signal.
- In the case of Globalstar interference towards Galileo, the receiver bandwidth is supposed equal to the width of the main lobe of the Galileo signal, and the interfering signal is assumed to be the aggregate of all 13 Globalstar channels. Note that this is also a worst case, as Globalstar channels are not active simultaneously all the time.

We should point out that ITU Recommendation M.1831 was developed primarily to be used for compatibility between RNSS systems using CDMA signals. But as Globalstar also uses CDMA signals, use of M.1831 should be an acceptable approach.

In order to avoid difficult coordination among terrestrial radio services, Globalstar stated that it operates below a specific

### Potential interference between Globalstar and hypothetical Galileo signals in S-band can be assessed through calculation of carrier-to-noise density ratio.

power flux density (PFD) threshold set in Table 5.2 of Appendix 5 of the Radio Regulations for the 2483.5–2500 MHz band. According to this, a maximum threshold value of  $-126$  dBW/m<sup>2</sup>/MHz per satellite must be considered.

For the purpose of assessing worst-case interference, we used the maximum PFD values for both Globalstar and Galileo satellites. As discussed in Part 1 of this column, the PFD levels calculated for various hypothetical Galileo signals in S-band are below the regulation's threshold except for the case of bi-phase shift key, BPSK(1), which at  $-122.78$  dBW/m<sup>2</sup>/MHz exceeds the tolerable value by slightly more than three decibels. This factor might indeed be a drawback for this signal option.

The other studied modulations do not exceed the PFD threshold because we did not consider the same transmitted power for all the modulations. Instead, as explained in Part 1, for each modulation we used the minimum transmitted power that would ensure the same thermal noise raw pseudo range error as the one obtained for E1-OS.

For the case of the interference caused by Galileo to Globalstar, we calculated the maximum accumulated PFD at the receiver antenna for a worst case, where 12 satellites are in view and the receiver gets the maximum power from all of them.

We also assumed a maximum receiver antenna gain of three decibels for all the satellites. Note that, although this is a pessimistic scenario, it enables us to set an upper-bound for the PFD.

We apply a similar assumption to the assessment of interference from Globalstar to Galileo; however, in this case, we fix the maximum number of Globalstar satellites simultaneously in view of a Galileo receiver at four.

In both interference cases, we must calculate the contributions from intra- and inter-system interferences in order to assess the degradation of the signal-to-noise ratio caused by the interfering system. We calculated interference, including SSC (inter-system) and self-SSC (intra-system), and then obtained the  $C/N_0$  degradation using expression (1) introduced previously.

Tables 1 through 5 present the results of our hypothetical interference analysis of the effects of Globalstar and Galileo on themselves and each other.

In order to calculate  $P_{max}$  from the maximum PFD of Globalstar, we needed to make some assumptions on the effective area of an isotropic receiving antenna. Assuming a zero-decibel gain and recalling that the effective area of the antenna and its gain have the relationship

$$A_e = \frac{G\lambda^2}{4\pi}$$

in which  $A_e$  is the effective area,  $G$  is the gain, and  $\lambda$  is the wavelength, we established an effective area of -29.4 dBm<sup>2</sup> for the receiving antenna in our calculations.

Note that some tables use the expression *maximum power spectral density (PSD)* [dBW/MHz], which is also often referred to in the literature as the *spectral adjustment factor (SAF)*. This term is widely used when calculating the *equivalent power flux density (EPFD)* of a given system.

Because Globalstar intra-system interference is low enough to be ignored, we have estimated the signal degradation due to the Galileo emissions alone and present them in Table 5. As can be seen from this table, Galileo just slight-

| Modulation Scheme of Desired Signal                            | CBOC(6,1,1/11) | BOC(1,1) | BPSK(1) | BPSK(4) | BPSK(8) |
|--|----------------|----------|---------|---------|---------|
| Globalstar Maximum PFD per satellite (dBW/m <sup>2</sup> /MHz) | -126           |          |         |         |         |
| Antenna effective area (dBm <sup>2</sup> )                     | -29.4          |          |         |         |         |
| Maximum PSD Globalstar – 1 satellite (dBW/MHz)                 | -11.14         |          |         |         |         |
| Maximum Received Power – 1 satellite (dBW)                     | -144.26        |          |         |         |         |
| Maximum number of satellites in view                           | 4              |          |         |         |         |
| Antenna Gain (dB)  | 3              |          |         |         |         |
| Implementation Loss (dB)                                       | 2              |          |         |         |         |
| Receiver bandwidth (MHz)                                       | 14.332         | 4.092    | 2.046   | 8.184   | 16.368  |
| SSC (dB/Hz)  | -72.21         | -72.67   | -72.46  | -72.42  | -72.36  |
| $I_o$ (dBW/Hz)   | -209.44        | -209.91  | -209.70 | -209.66 | -209.6  |

TABLE 1. Interference noise density  $I_o$  caused by Globalstar emissions into GNSS

| Modulation Scheme of Desired Signal                | CBOC(6,1,1/11) | BOC(1,1) | BPSK(1) | BPSK(4) | BPSK(8) |
|--|----------------|----------|---------|---------|---------|
| Galileo Minimum Received Power – 1 satellite (dBW) | -157.25        |          |         |         |         |
| Maximum number of satellites in view               | 12             |          |         |         |         |
| Antenna Gain (dB)                                  | -3             |          |         |         |         |
| Implementation Loss (dB)                           | 2              |          |         |         |         |
| Receiver bandwidth (MHz)                           | 14.332         | 4.092    | 2.046   | 8.184   | 16.368  |
| Self-SSC (dB/Hz)                                   | -65.50         | -64.81   | -61.84  | -67.76  | -70.67  |
| $P_o$ (dBW/Hz)                                     | -216.96        | -216.27  | -213.30 | -219.22 | -222.13 |

TABLE 2. Galileo Intra-System Interference Noise Density  $P_o$

|                          | CBOC(6,1,1/11) | BOC(1,1) | BPSK(1) | BPSK(4) | BPSK(8) |
|--------------------------|----------------|----------|---------|---------|---------|
| $I_o$ [dBW/Hz]           | -209.44        | -209.91  | -209.70 | -209.66 | -209.6  |
| $P_o$ [dBW/Hz]           | -216.96        | -216.27  | -213.30 | -219.22 | -222.13 |
| $N_o$ [dBW/Hz]           | -201.5         |          |         |         |         |
| $C/N_o$ degradation [dB] | 0.63           | 0.57     | 0.58    | 0.61    | 0.62    |

TABLE 3. Galileo  $C/N_o$  degradation due to Globalstar Emissions

| Modulation Scheme of Interfering Signal                     | CBOC(6,1,1/11) | BOC(1,1) | BPSK(1) | BPSK(4) | BPSK(8) |
|---|----------------|----------|---------|---------|---------|
| Galileo Maximum pfd per satellite (dBW/m <sup>2</sup> /MHz) | -126           |          |         |         |         |
| Antenna effective area (dBm <sup>2</sup> )                  | -29.4          |          |         |         |         |
| Maximum PSD Galileo – 1 satellite (dBW/MHz)                 | -5.25          | -4.84    | -3.11   | -6.37   | -9.19   |
| Maximum Received Power – 1 satellite (dBW)                  | -150.15        | -150.56  | -152.29 | -149.03 | -146.21 |
| Maximum number of satellites in view                        | 12             |          |         |         |         |
| Antenna Gain (dB)   | 3              |          |         |         |         |
| Implementation Loss (dB)                                    | 2              |          |         |         |         |
| Receiver bandwidth (MHz)                                    | 1.23           |          |         |         |         |
| SSC (dB/Hz)   | -78.20         | -77.85   | -72.74  | -77.13  | -79.84  |
| $I_o$ (dBW/Hz)  | -216.56        | -216.21  | -211.10 | -215.49 | -218.20 |

TABLE 4. Interference noise density  $I_o$  due to Galileo emissions

|                          | CBOC(6,1,1/11) | BOC(1,1) | BPSK(1) | BPSK(4) | BPSK(8) |
|--------------------------|----------------|----------|---------|---------|---------|
| $I_o$ (dBW/Hz)           | -216.56        | -216.21  | -211.10 | -215.49 | -218.20 |
| $N_o$ (dBW/Hz)           | -201.5         |          |         |         |         |
| $C/N_o$ degradation (dB) | 0.13           | 0.14     | 0.45    | 0.17    | 0.09    |

TABLE 5. Globalstar  $C/N_o$  degradation due to Galileo emissions

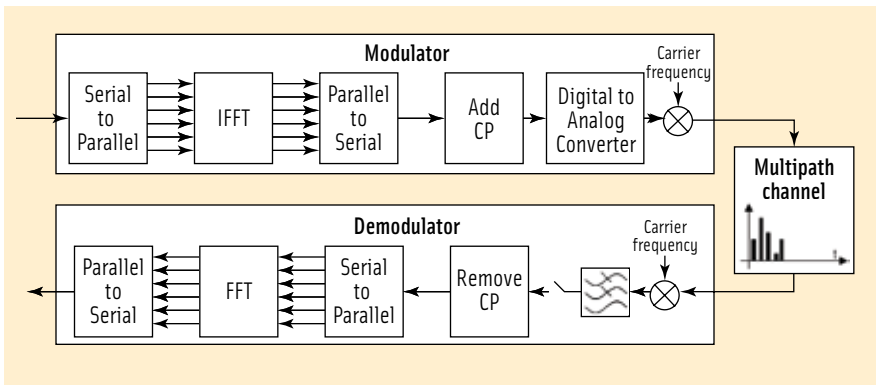


**FIGURE 1** Basic OFDM transmission/reception chain (From the article by P. Thevenon et alia 2009a listed in Additional Resources)

ly degrades Globalstar's  $C/N_0$  and the maximum degradation is 0.45 decibel in the case of the BPSK(1) modulation, while for all the other cases it is limited to about 0.1 decibel. However, in the reciprocal case, Globalstar degrades the Galileo signal by almost 0.6 decibel in all the cases, with results shown in Table 3.

Taken as a whole, these results indicate that, in all cases, the interference between the two systems stays within very reasonable values, and that we should not expect a new Galileo signal in S-band to be an issue from an RF compatibility perspective.

## Interference with Other Services

The 2483.5–2500 MHz band is used also for mobile services (MS) systems. Our calculations for radio determination satellite service (RDSS)/MS radio frequency compatibility indicate that only for a few GNSS signal options presented previously the intersystem interference criteria might be exceeded, and that even for those exceptional cases, interference to Globalstar caused by the Galileo signal is below that induced by Globalstar into GNSS.

Because no other internal compatibility problems between Globalstar and other mobile services have been reported, we conclude that the interference criterion considered is, in reality, far too conservative. Thus, the introduction of any of the presented modulations in S-band is not expected to cause harmful interference to any MS system.

The 2483.5–2500 MHz band is also planned for the deployment of future Worldwide Interoperability for Microwave Access (WiMAX) services. WiMAX service will have to be compatible with the signals already present in the band, and particularly with Globalstar.

Our computations show that the estimated interference on Globalstar due to WiMAX are similar to those due to Galileo. Accordingly, we believe that if WiMAX signals are robust enough to survive Globalstar interference, they should also be sufficiently robust against any hypothetical additional Galileo signal.

Fixed service allocations also exist in S-band, specifically from 2450 to 2690 MHz. These services consist of long range point-to-point links between two highly directive antennas. Again, our computations show that no additional limitation needs to be imposed on the RDSS PFD in order to prevent harmful interference with fixed services.

Future work will address the criteria needed to assess compatibility between several systems in a common band, including both the criteria of  $C/N_0$  degradation and effective  $C/N_0$ .

## Another Modulation Option: OFDM

Orthogonal frequency division multiplexing (OFDM) is a modulation technique used for numerous existing and forthcoming telecommunications and broadcasting standards, such as WiFi, WiMAX, digital video broadcasting

(DVB-T, DVB-H, DVB-SH), and digital audio broadcasting (DAB).

The technique consists of transmitting data symbols over several orthogonal narrow-band subcarriers, for example, one symbol per subcarrier. In the latter case, each subcarrier is chosen such that it is narrow enough that the channel response can be considered as flat over the width of the subcarrier. Therefore, the impact of the propagation channel on the signal can be easily corrected using simple channel equalization techniques.

The narrowness and orthogonality of the subcarriers ensure excellent spectral efficiency with the signal PSD being almost rectangular. Even with a low symbol rate, a large number of subcarriers transmitted in parallel guarantees a high global data rate.

The digital implementation of OFDM makes use of an efficient fast Fourier transform (FFT) algorithm. An OFDM symbol is generated by passing  $N$  data symbols through the inverse-FFT and results in the generation of  $N$  samples of the OFDM symbol to be transmitted. Reciprocally, the  $N$  data symbols are recovered through the FFT of the  $N$  received samples of an OFDM symbol.

Additionally, a guard interval is added in front of the OFDM symbol in order to avoid interference between two consecutive OFDM symbols. In general, this guard interval exactly replicates the end of the OFDM symbol. In this case, it is usually referred to as *cyclic prefix* (CP). Thus, even if the FFT window begins within the CP, the data symbols are properly recovered and only affected by a phase rotation. As a result, data demodulation does not require precise timing synchronization.

A block diagram of the basic OFDM transmission/reception chain is presented in **Figure 1**.

Thanks to the presence of the CP and the use of simple channel equalization techniques, OFDM modulation can be used in synchronized single-frequency networks (SFN), where all emitters broadcast the same signal in the same frequency band.

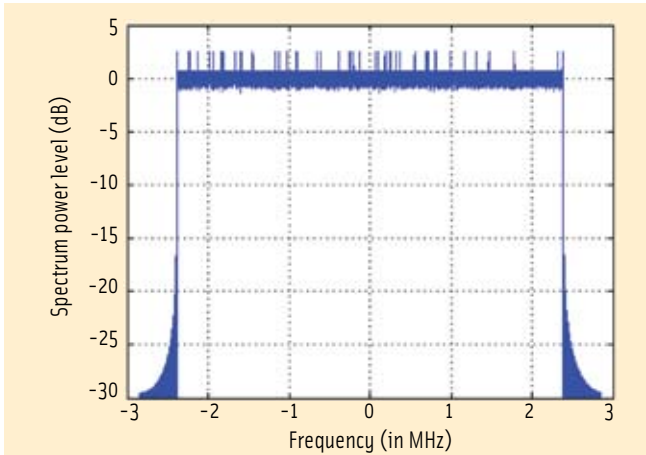


FIGURE 2 Power spectral density of a DVB-SH OFDM signal in S-band

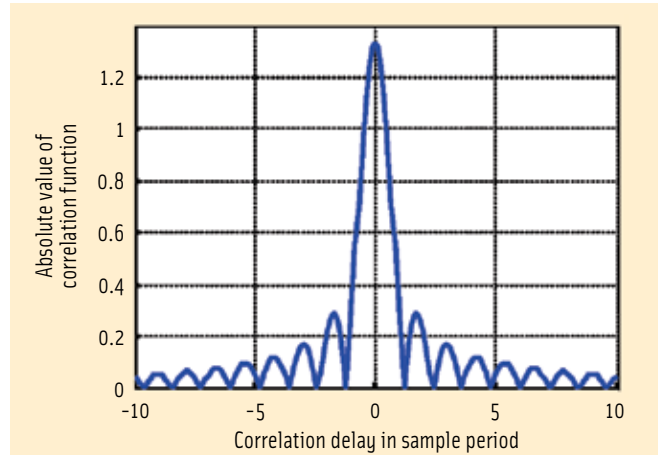


FIGURE 3 Correlation function used by the proposed DLL (1 sample period equals 175 nanoseconds)

To properly demodulate the transmitted data, the receiver has to perform several operations:

- rough timing synchronization to ensure that the FFT window starts at the beginning of the OFDM symbol or at the end of the CP
- fine frequency synchronization to maintain the sub-carrier orthogonality, thus avoiding *inter-carrier interference* (ICI), and
- channel equalization to compensate for the channel effects, thus improving the data demodulation performance.

Generally, an OFDM symbol contains several pilot sub-carriers that carry known data symbols. These pilot sub-carriers ease the *channel impulse response* (CIR) estimation and thus the equalization.

### OFDM Potential for Navigation

In order to investigate the potential of OFDM signals for navigation and, in particular, their ranging capability, this section presents a case study of the existing digital video broadcasting — satellite to handheld (DVB-SH) standard.

The European Telecommunications Standards Institute (ETSI) developed the DVB-SH standard for the transmission of mobile TV signals in S-band. The combination of ground stations with geostationary satellites in a synchronous SFN is planned, while current research activities are assessing the use of this

standard to provide signals of opportunity for positioning.

Figure 2 illustrates the power spectral density of a representative DVB-SH signal using 2,048 sub-carriers and a bandwidth of 4.75 megahertz. In this case, the PSD has very low out-of-band emissions. Each DVB-SH subcarrier transmits one of several types of symbols, including:

- Null data in which 343 null subcarriers at the band edge ensure band limitation (the number of sub-carriers being a power of 2).
- Payload data — TV data for the DVB-SH standard
- transmission parameter information
- known pilot symbol used for CIR estimation, which is particularly interesting for navigation because it enables computation of a pseudorange. (These pilot sub-carriers occupy about 10 percent of the useful sub-carriers and are transmitted

at boosted power. This is why several peaks can be seen in Figure 2.)

The articles by P. Thevenon et alia (2009b) and D. Serant *et alia* listed in the Additional Resources section near the end of this article present a positioning principle using DVB-SH signal in a terrestrial SFN. In these studies, pseudorange measurements are obtained by using a delay locked loop (DLL) in which the local replica is a DVB-SH signal with only the pilot subcarriers activated, with the remaining subcarriers set to zero.

Due to the rectangular shape of the OFDM spectrum, the correlation function used by the DLL is a sine function, as presented in Figure 3. The tracking process is summarized in Figure 4.

The theoretical standard deviation of the tracking error in white noise, derived by D. Serant *et alia*, is illustrated in Figure 5 assuming 2,048 sub-carriers (including 142 pilot sub-carriers), a signal bandwidth of 4.75 megahertz,

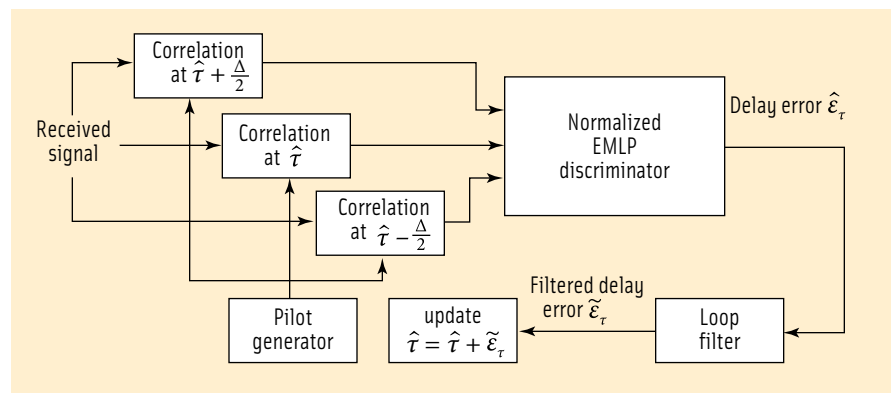


FIGURE 4 Tracking diagram

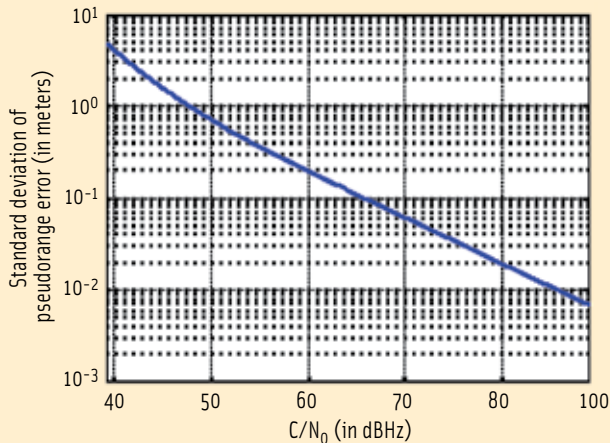


FIGURE 5 Tracking error standard deviation versus  $C/N_0$

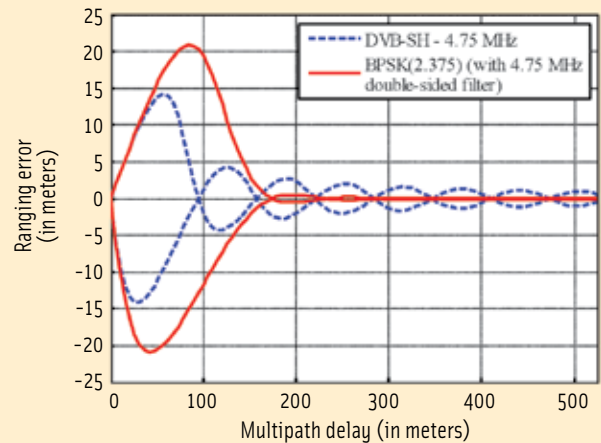


FIGURE 6 Multipath error envelope, correlator spacing of 175 nanoseconds — equivalent to 0.41 chip for the BPSK(2.375)

an equivalent DLL loop bandwidth of 10 Hertz, and correlator spacing equal to 175 nanoseconds. This performance is lower than that of a BPSK(2.375) signal (the main lobe of which would occupy the same bandwidth as the OFDM signal). Moreover, Serant *et alia* showed that the influence of the correlator spacing on the tracking error was very limited, exhibiting the following characteristics:

- Correlation gain improves when a higher number of pilot subcarriers is used, thus becoming more similar to the tracking performance of a BPSK signal. For instance, in order to emulate a case where all the subcarriers are pilot subcarriers, the same data can be transmitted on all — or a large number of — subcarriers.
- The OFDM modulation allows minimum out-of-band (OoB) emissions compared to BPSK, an important characteristic in the case particular OoB constraints would be required for S-band transmissions.

The multipath error envelope is detailed in Figure 6. The multipath is considered to have an amplitude half of the Line-of-Sight (LOS). The same parameters as in the previous figure are used to calculate the multipath delay. Here, the multipath error envelope of the DVB-SH signal is compared against a BPSK(2.375) signal filtered so that only the main lobe remains.

This comparison is made to reproduce the case of a necessarily stringent

band limitation. The same correlator spacing is used for both cases. It can be observed that the DVB-SH envelope is smaller than that of the BPSK(2.375). However, the DVB-SH oscillates over long-delay multipath due to the secondary lobes of the correlation function, which is a consequence of the natural band limitation of the OFDM signal.

This OFDM-based ranging capability combined with the potential use of emitters in a synchronized SFN could present an interesting option within a GNSS positioning system.

### OFDM Summary

OFDM signals are spectrally efficient and can provide reasonable performance

integrity, data aiding, messages, other data channels, and so forth — and/or navigation data including ephemerides, almanacs, and other reference data.

We recommend further study of the usage of OFDM modulation for navigation signals. Relevant subjects that remain to be addressed include:

- The issue of the emitter's discrimination in an SFN. In order to address this problem, the MC-CDMA modulation discussed in the article by S. Hara and R. Prasad could be investigated.
- The sharing of bandwidth between the telecommunication data and the pilot data used for navigation can be adapted to a desired configuration, depending on the balance between

**If a totally new signal is designed for combining telecommunication and navigation services . . . then the OFDM modulation could be an interesting candidate.**

in terms of ranging capability. If a totally new signal is designed for combining telecommunication and navigation services with a high constraint in terms of out-of-band emissions, then the OFDM modulation could be an interesting candidate.

OFDM could allow for an efficient use available bandwidth, supporting communication services as well as GNSS and thus enabling the addition of other capabilities — location based services,

the two services. For example, more pilots would improve tracking at the expense of telecom capacity.

- OFDM is known to have a high peak-to-average power ratio, which creates heavy non-linear distortion introduced by the satellite on-board high power amplifier. This issue can be addressed by using coding or pre-distortion techniques in order to reduce the PAPR. Considering moreover that the bands

above 2.5 GHz are mobile bands and likely to be used for either WiMAX or 3G LTE (both of which use OFDM techniques), the use of OFDM for an S-band navigation signal baseline becomes even more interesting.

**Conclusions**

The potential benefits of a future Galileo S-band in terms of performance and

frequency compatibility are many. Those benefits include the capability of multiple new RNSS signals and services sharing the band, as well as combining mobile satellite communications solutions with typical navigation approaches.

In this two-part column, we have assessed various exemplary signals to prove the concept, and we recommend further research.

Performance improvement alone does not drive the addition of new frequencies for GNSS, but rather provides an opportunity to serve user groups currently lacking the performance they need with the current RNSS signals provided by L-band.

Several frequency band options are being studied in the framework of the evolution of Galileo. Assuming a new

**Globalstar Signal**

Globalstar uses the 2483.5–2500 MHz band for its downlink communications between the satellite and user terminals. The system uses multi-beam antennas to allow frequency reutilization. In every beam, the 16.5 MHz bandwidth is divided into 13 FDMA channels, each 1.23 MHz wide, as shown in the **Figure 1**.

Code division multiple access (CDMA) with a chipping rate of 1.2288 Mcps is implemented inside every FDMA channel. Walsh codes 128 chips long are used to distinguish the users, which gives 128 orthogonal codes per channel. The data + Walsh code stream is first modulated by an outer pseudo-random noise (PRN) sequence at 1.2 kcps. An inner PRN sequence pair is then used to get a quadrature phase shift keying (QPSK) modulation, as shown in **Figure 2**.

One inner PRN sequence period exactly fits into a single outer PRN chip. The outer PN modulates the inner PRN sequence to produce the actual spreading sequence resulting

in a period of 240 milliseconds (288 chips of the outer PRN sequence).

The inner PRN sequence pair identifies the satellite orbital plane, resulting in eight different pairs. Thus all the satellites on a same orbital plane have the same inner PRN sequence. The outer PRN sequence identifies the satellite, and finally, each satellite beam is identified by a different time offset of the outer PRN sequence.

Before modulation of the carrier, both I and Q components are filtered by a Nyquist-square-root raised-cosine (SRC) filter with roll-off factor,  $\rho=0.2$ . The use of the SRC filter yields the following power spectral density (PSD) for a given  $k^{th}$  frequency division multiple access (FDMA) channel in baseband:

$$G_{SRC}^k(f) = \begin{cases} 1 & \text{if } |f - kB| \leq \frac{f_c}{2}(1 - \rho) \\ 0 & \text{if } |f - kB| \geq \frac{f_c}{2}(1 + \rho) \\ g(f) & \text{if } \frac{f_c}{2}(1 - \rho) \leq |f - kB| \leq \frac{f_c}{2}(1 + \rho) \end{cases}$$

where

$$g(f) = 1 + \cos\left(\frac{\pi}{\rho f_c} \left(|f| - \frac{(1 - \rho)f_c}{2} - kB\right)\right)$$

- $f_c = 1.2288$  Mcps is the chip rate,
- $B = 1.23$  MHz is the bandwidth of a single FDMA channel,
- $P$  is the roll-off factor.

Finally, the whole Globalstar signal PSD can be expressed as the sum of the PSDs of the 13 FDMA channels, such that

$$G_{GLOB}(f) = \sum_{k=-6}^6 G_{SRC}^k(f)$$

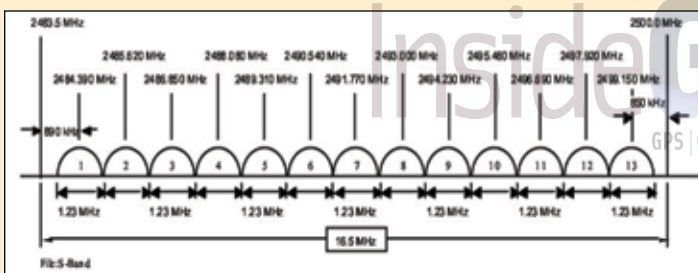


FIGURE 1 Globalstar FDMA scheme

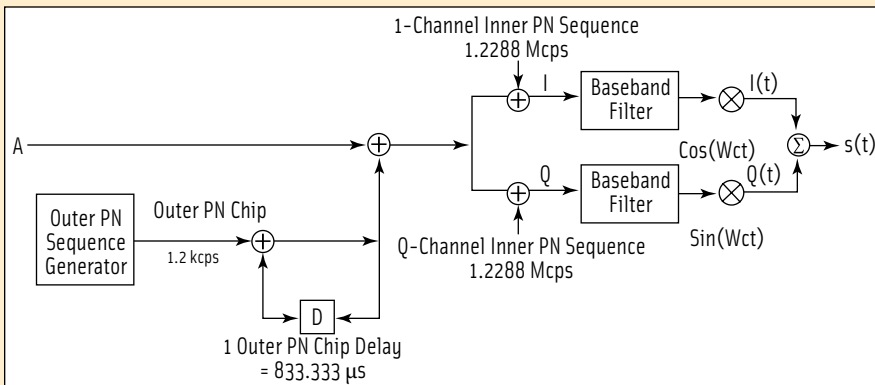


FIGURE 2 Generation of the Globalstar signal

service would be identified for a future GNSS system, no matter what the final selected signal would be, backward compatibility with legacy modulations is essential for legacy users.

Radio frequency compatibility between S-band RDSS systems, Globalstar, and other terrestrial mobile or fixed services seems to be possible. In the next 5 to 10 years, if the L1 band continues to be occupied by more and more RNSS systems, worst-case C/N0 degradation on the order of 2.5 decibels could occur, without even taking into consideration the effect of non-RNSS interference in L1.

In such a scenario, the potential addition of GNSS signals in S-band looks promising. However, further detailed studied is needed, addressing all necessary signal design criteria and design trades among the various new frequency options. These include GNSS S-band modulation methods such as BPSK, BOC, MBOC, OFDM, and other solutions. In this context, to support potential future signals in S-band, a Galileo 2 filing including the 2.5 GHz band is available for review on the ITU website.

## Disclaimer

The authors would like to make it clear that Europe has not yet decided on use of an additional RF band — e.g., S-band — for the second generation of Galileo, other than to ensure that any future frequency plan is backward-compatible with the system's current navigation signals. Accordingly, this column should be considered as a scientific exercise that only emphasizes the great interest in considering use of this band for GNSS systems.

## Additional Resources

[1] *International Telecommunications Union Recommendation, ITU-R M.1831, "A coordination methodology for RNSS inter-system interference estimation,"* 2007

[2] European Telecommunications Standard Institute ETSI EN 302 583, "Digital Video Broadcasting (DVB); Framing Structure, channel coding and modulation for Satellite Services to Handheld devices (SH) below 3 GHz," 2008

[x] Thevenon P., (2009a) and O. Julien, C. Macabiau, D. Serant, S. Corazza, M. Bousquet, . Pseudo-Range Measurements Using OFDM Channel Estimation, Proceedings of the ION GNSS 2009, pp. 481-493, 2009

[3] Thevenon, P., (2009b) and O. Julien, D. Serant, L. Ries, S. Corazza, et al., "Positioning principles with a mobile TV system using DVB-SH signals and a Single Frequency Network," *16th Conference on Digital Signal Processing*, 2009

[4] Serant, D., and O. Julien, C. Macabiau, P. Thevenon, M. Dervin, S. Corazza, L. Ries, and M. L. Boucheret, "Development and Validation of an OFDM/DVB-T Sensor for Positioning," *IEEE/ION PLANS*, 2010

[5] Hara, S., and R. Prasad, "Overview of Multi-carrier CDMA," *Communications Magazine, IEEE*, vol.35, no.12, pp.126-133, December 1997

[6] Cioni, S., and G. E. Corazza, M. Neri, and A. Vanelli-Coralli, "On the use of OFDM Radio Interface for Satellite Digital Multimedia Broadcasting Systems," *International Journal of Satellite Communications and Networking*, vol. 24, no. 2, pp. 153-167

[7] Bingham, J.A.C., "Multicarrier modulation for data transmission: An idea whose time has come," *IEEE Communications*, vol. 28, 1990

[8] Godet, J. "GPS/GALILEO Radio Frequency Compatibility Analysis," ION GPS, 2000

[9] de Gaudenzi, R., "Payload Non-linearity Impact on the Globalstar Forward Link Multiplex. Part I. Physical Layer Analysis," *IEEE Transactions on Vehicular Technology*, vol. 48, no. 3, May 1999

[10] L. Schiff, L., and A. Chockalingam, "Design and System Operations of Globalstar versus IS-95 CDMA, Similarities and Differences," *Wireless Network*, 6:47-57, 2000

## Manufacturers

The data presented in this article was plotted using MATLAB from **The Mathworks, Inc.**, Natick, Massachusetts, USA. Globalstar satellite services are provided by **Globalstar**, Milpitas, California, USA.

## Authors



Isidre Mateu graduated in telecommunications engineering from the Universitat Politècnica de Catalunya. He currently works as a navigation engineer in the French Space Agency (CNES) Signal and Radio-

navigation Department, and collaborates with the ESA-CNES integrated team for EGNOS evolutions.



**Matteo Paonni** is research associate at the Institute of Geodesy and Navigation at the University of the Federal Armed Forces Munich, Germany. He received his B.S. and M.S. in electrical engineering from the University of Perugia, Italy. He is involved in several European projects that focus on GNSS. His main topics of interest are GNSS signal structure, GNSS interoperability and compatibility, and GNSS performance assessment.



**Jean-Luc Issler** is head of the Instrumentation Telemetry/telecommand and Propagation (ITP) department of the CNES Radiofrequency sub-directorate since August

2009. He is one of the inventors of CBOC and proposed the Galileo E5 signal using the AltBOC 8-PSK invention made by Laurent Lestarquit. Issler graduated from the Ecole Supérieure d'Electronique de l'Ouest (ESEO). He received the Astronautic Prize French Aeronautical and Astronautic Association in 2004, as well as the EADS Science and Engineering prize awarded in 2008 by the French Academy of Sciences for his work on GNSS frequencies and modulations, and space-borne RF equipment.



**Guenter W. Hein** is head of the Galileo Operations and Evolution Department of the European Space Agency. Previously, he was a full professor and director of the

Institute of Geodesy and Navigation at the University FAF Munich. In 2002 he received the prestigious Johannes Kepler Award from the U.S. Institute of Navigation (ION) for "sustained and significant contributions to satellite navigation." He is one of the CBOC inventors.

[Editor's note: biographies of additional authors will be made available on-line at <insidegnss.com>.)